Direct Measurement of Diffuse Double-Layer Forces at the Semiconductor/Electrolyte Interface Using an Atomic Force Microscope

Kai Hu, Fu-Ren F. Fan, and Allen J. Bard*

Department of Chemistry and Biochemistry, University of Texas at Austin, Austin, Texas 78712

Andrew C. Hillier*

Department of Chemical Engineering, University of Virginia, Charlottesville, Virginia 22903

Received: June 10, 1997; In Final Form: August 5, 1997[⊗]

The forces between a silica probe and an n-type TiO_2 single-crystal electrode were measured using an atomic force microscope in an aqueous electrolyte solution. These interactions were a strong function of the solution pH, the presence of specifically adsorbed anions, and the TiO_2 electrode potential. For a series of pH values, a strong electrostatic repulsion was seen at high pH and decreased as the pH was reduced. At pH values below 5.5, the interaction became attractive. A series of force measurements between SiO_2 and n-type TiO_2 showed a repulsive interaction when TiO_2 was held at negative electrode potentials, which transformed to an attractive force at positive potentials. The potential at which the interaction passed through a minimum, called the potential of zero force (pzf), corresponded closely to the flat-band potential (V_{fb}) of the TiO_2 electrode under conditions where the solution pH was held at the isoelectric point (iep) of titania. The V_{fb} measured by this method gave a value near −0.4 V vs SCE at pH 5.5, which was in good agreement with photoelectrochemical measurements made under similar conditions. At pH values deviating from the iep, the pzf and V_{fb} were not equivalent. This was illustrated by potential- and pH-dependent force curves taken at the same n-TiO_2 electrode in the presence of the polymeric anion hexametaphosphate (HMP), which is known to specifically adsorb on TiO_2. An increase in negative surface charge due to adsorbed HMP was observed by an increase in the repulsive force with respect to the silica probe at open circuit for a specific pH value. Potential-dependent force measurements determined that the pzf shifted toward more positive values in the presence of HMP, in direct opposition to the negative shift in V_{fb}. This apparent discrepancy was caused by the presence of both adsorbed and potential-induced surface charge, which could not be differentiated by simply measuring the diffuse double-layer charge.

Introduction

Surface forces and double-layer phenomena play an important role in numerous interfacial processes including colloidal stability, polyelectrolyte adsorption, ion partitioning in biological and polymer membranes, and electrochemical processes. Recent advances in the development of techniques allowing accurate and high-resolution measurement of surface forces have provided insight into this interface at a level that allows direct comparison to theory and the ability to directly detect phenomena associated with diffuse double-layer charge, solvent and solute ordering forces, nanoscale tribology, and molecular adsorption.[1]

The measurement of surface forces is typically achieved using the surface forces apparatus (SFA)[2] or the total internal reflectance microscope.[3] However, the atomic force microscope (AFM) has received increasing attention as a tool for performing surface force measurements because of its versatility and ability to perform force measurements with both high normal and lateral resolution.[4] The measurement of colloidal forces with AFM was initially demonstrated between silica surfaces by Ducker, Senden, and Pashley,[5] who functionalized a standard AFM tip with a spherical silica probe to measure the interaction between silica surfaces. Recently, AFM has been used to measure surface forces at a variety of colloidal materials, including semiconductors,[6] polymers,[7] and metals[8] as well as in the presence of surfactant[9] and polymer[10] adsorbates.

The presence of electrical double layers at electrode surfaces plays an important role in electrochemical processes. Although the direct measurement of these double layers at electrode surfaces has been somewhat limited, an early examination of the force between two metal wires in an electrolyte solution illustrated a potential-dependent repulsive force.[11] More recent studies of this interface include the examination of thin-layer cell behavior[12] and electrostatic forces[13] between two platinum-coated mica surfaces with the SFA. The AFM has recently proven successful in directly measuring the magnitude and potential dependence of diffuse double-layer forces at electrode surfaces.[14,15] These measurements provide direct experimental information about the magnitude and structure of the diffuse double layer, which could previously only be examined indirectly through surface tension or electrocapillary measurements at liquid (Hg) electrodes[16] or capacitance studies at liquid and metal electrodes.[17]

Although electrostatic forces at semiconductor surfaces have previously been examined,[6] the influence of electrochemical variables in these systems has not been addressed. In this report, we describe how the diffuse double layer at an n-type TiO_2 single-crystal electrode can be probed at nanometer resolution with the AFM. The double layer was examined by measuring the force between a spherical silica probe placed on the end of an AFM cantilever and a TiO_2 substrate as the probe moved through the double layer (Scheme 1). The charge residing within the diffuse double layer, which reflects charge present at the semiconductor surface, is calculated from the force between the electrode and the tip of the AFM cantilever. Results

* To whom correspondence should be addressed.

[⊗] Abstract published in *Advance ACS Abstracts,* September 15, 1997.

S1089-5647(97)01887-7 CCC: $14.00

SCHEME 1: Representation of AFM Force Measurement between a Negatively Charged Silica Sphere and a TiO_2 Substrate in an Aqueous Solution

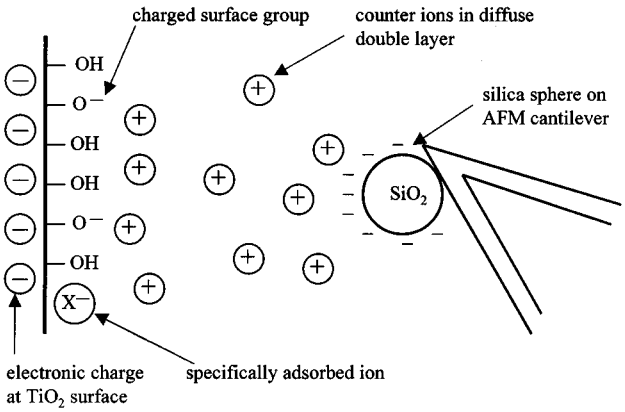

indicate that these forces are a strong function of the solution pH and the potential applied to the TiO_2 electrode. In circumstances where the adsorption-induced surface charge is zero, which occurs at the isoelectric point (iep), the electrode potential at which the interaction force drops to zero, referred to as the potential of zero force (pzf), corresponds closely to the flat-band potential (V_{fb}). Under conditions deviating from the iep, where both potential- and adsorption-induced charges exist on the TiO_2 surface, the pzf and V_{fb} do not correspond and are actually shifted in opposite directions. This is illustrated for the adsorption of the polymeric anion hexametaphosphate (HMP) on TiO_2.

Experimental Section

Materials. *Reagents.* Solutions of KCl were prepared from reagent grade chemicals (Aldrich, Milwaukee, WI) in 18 MΩ deionized water (Milli-Q Plus, Millipore Corp., Bedford, MA). Sodium hexametaphosphate (HMP, $(NaPO_3)_n$) was used as received (Alfa, Ward Hill, MA). Solution pH values were adjusted by adding 0.01 M NaOH or 0.01 M HCl. Immediately prior to use, the solutions were deaerated with argon for 30 min to achieve stable pH values.

Probe Preparation. Force measurements were acquired using a microfabricated AFM cantilever that had been functionalized with a silica sphere in a fashion similar to the procedure of Ducker, Senden, and Pashley.[5b] A silica sphere with nominal diameter of 10−20 μm (Polysciences, Warrington, PA) was attached to the tip of a commercially available AFM cantilever (Nanoprobe, Park Scientific, Mountain View, CA) using thermal-setting epoxy resin (Epon 1002, Shell, Houston, TX) and an optical microscope with three-dimensional positioning capabilities (Olympus, Model BHTU, Tokyo, Japan).[15] Force measurements using a standard cantilever with integral, square-pyramidal tips suffered from an ill-defined interaction radius and a much smaller signal-to-noise ratio. Immediately prior to use, the force-sensing tip was rinsed with ethanol, rinsed with purified water, and blown dry with nitrogen.

Substrate Preparation. Silica substrates were prepared from commercial glass cover slips that were cleaned in a concentrated sulfuric/nitric acid solution prior to exposure to condensing steam vapor for 30 min. AFM imaging of the silica surfaces showed a mean roughness of 1.1 nm/μm^2 with a maximum peak-to-valley height of 3.7 nm over a 1 × 1 μm^2 area as determined by AFM imaging.

The TiO_2 electrode was cut perpendicular to the C_2 axis from a rutile single crystal. n-type semiconductivity was achieved by heating in hydrogen at 700 °C for 30 min. Electrical contact was made by connecting a copper wire to the backside of the TiO_2 electrode using Ga−In eutectic. The TiO_2 electrode was then mounted to a magnetic, stainless steel AFM sample disk with epoxy (Torr Seal, Varian). The electrode surface was polished to optical smoothness using successively finer grades of diamond and alumina paste (15, 6, 3, 1, 0.3, and 0.05 μm; Buehler, Lake Bluff, IL). The electrochemically active electrode area was 0.1 cm^2, and the surface exhibited a mean roughness of 0.8 nm/μm^2 with a maximum peak-to-valley height of 3.4 nm over a 1 × 1 μm^2 area. Prior to use, the TiO_2 was sonicated for 15 min to remove any polishing particles followed by steam cleaning with Milli-Q water for 2 h to remove any surface contaminants. The electrode was then rinsed in ethanol and copious amounts of purified water and blown dry under argon.

Electrochemistry and Force Measurements. *Equipment.* Force measurements were performed with a Nanoscope III scanning probe microscope (Digital Instruments, Santa Barbara, CA) equipped with silicon nitride cantilevers (Nanoprobe, Park Scientific, Mountain View, CA) having integral, bipyramidal tips. The tips were modified by the attachment of a spherical silica bead as described earlier.

Experiments were carried out in a fluid cell (Digital Instruments) with Teflon tubing. A three-electrode design was used for electrochemical measurements with the TiO_2 crystal serving as the working electrode, a Pt counter electrode, and a SCE reference electrode. The counter and reference electrodes were placed in a saturated KCl solution, which was connected through a salt bridge to the outlet of the fluid cell. All electrode potentials are given with respect to this SCE reference. Electrochemical control of the cell was effected with a PAR 173 potentiostat and 175 universal programmer (EG&G Instruments, Princeton, NJ).

Force Measurements. The cantilever spring constant k was determined using a published procedure.[18] A series of end masses were added to the tip, and the change in the cantilever's resonance frequency was recorded. This method provided a spring constant of 0.65 ± 0.12 N m^{-1} for the cantilevers used here. Force−separation curves were obtained by recording the voltage from the split photodiode detector and the substrate displacement as given by the applied piezovoltages. The photodiode voltages and piezovoltages were converted via calibration standards to normalized force (force/radius) versus tip−substrate separation for further analysis.

Flat-Band Potential Measurements. The flat-band potential of the same n-type TiO_2 single-crystal electrode was measured by photocurrent onset potential and open-circuit photovoltage methods in 10^{-3} and 10^{-4} M KCl solutions at pH 5.5. A Christie Xenolite UF30KK illuminator (Christie Electric Corp., Los Angeles, CA) with a 2500 W xenon/mercury lamp operating at 1500 W was used as the illumination source in the photoelectrochemical measurements. The output was filtered through 18 cm of H_2O to remove infrared light and was focused onto the TiO_2 electrode surface through a quartz window. In the photocurrent onset potential experiments, dark and photocurrent voltammograms were recorded with a PAR 173 potentiostat and a PAR 175 universal programmer. In the open-circuit photovoltage measurements, the open-circuit photovoltage was taken to be the difference between the rest potential in the dark and under illumination. In all cases, a SCE reference electrode was used.

Results and Discussion

Theory. Theories describing the forces between interacting double layers in electrolyte solutions are well-developed. For identically charged surfaces at small surface potentials, the interaction is adequately described by the theory of Derjaguin−Landau−Verwey−Overbeek (DLVO).[19] Using the Derjaguin

approximation,[20] the force between two spheres of effective radius R_T can be related to the energy between two plates by the expression

$$F/R_T = 2\pi(V_A + V_E + V_S) \quad (1)$$

V_A is the van der Waals interaction energy which, in the nonretarded limit, is given by the form

$$V_A = -A_H/12\pi d^2 \quad (2)$$

where A_H is the Hamaker constant and d is the separation distance. For this work, the term V_S, which is associated with the ordering of solvent layers, is neglected. This term is often described by a decaying oscillatory function.[21] The electrostatic term (V_E) can be derived by integrating the electrostatic force between two charged surfaces according to

$$V_E = \int_\infty^d \left\{2n^0 kT\left[\cosh\left(\frac{ze\psi}{kT}\right) - 1\right] - \frac{\epsilon}{2}\left(\frac{d\psi}{dz}\right)^2\right\} dz \quad (3)$$

where ψ is the electrostatic potential. To determine V_E explicitly, the electrostatic potential must be known. This can be found by solving the Poisson−Boltzmann equation

$$\frac{d^2\psi}{d^2z} = -\frac{1}{\epsilon_0\epsilon_r}\sum n_i^0 z_i e \exp\left(-\frac{z_i e\psi}{kT}\right) \quad (4)$$

which describes the electrostatic potential between two charged plates in an electrolyte solution. Although linearized forms of eq 4 can be solved analytically for low potentials, the complete nonlinear form of eq 4 can only be solved numerically. In this work, a finite element discretization of eq 4 was performed with linear basis functions. Integration of eq 3 was then achieved with Simpsons' 3/8 rule. Details of this calculation have been provided previously.[15]

This model of the interaction force between two charged surfaces has proven extremely successful in matching experimental observations for a variety of systems for separations ranging down to the last 3−5 nm. Below these small separations, nontrivial surface roughness introduces uncertainties in the location of the plane of surface charge and introduces a nonideality in the model spherical surface geometry. The solvent force also begins to become important under these conditions. Also, the application of this model to a semiconductor/electrolyte interface is somewhat of a simplification. Although it has been successful in modeling the potential-dependent behavior of a metal electrode,[15] this model neglects the potential drop associated with the semiconductor's space-charge layer. However, in this work, the electrolyte concentration was kept at a low level, and the semiconductor was highly doped such that the thickness of the semiconductor depletion layer was much smaller than the diffuse double layer. Under these conditions, the proposed model is a reasonable assumption that converges to the complete solution as the flat-band potential is approached.

Force Measurements. The interaction between SiO_2 surfaces is fairly well established.[5,22] In aqueous solutions under conditions where the solution pH exceeds the iep of silica (∼2), the surface is negatively charged. In an electrolyte solution, this produces a diffuse double layer with excess positive charge due to the accumulation of excess positive ions in solution near the SiO_2 surface. The resulting electrostatic interaction between two SiO_2 surfaces is strictly repulsive, with a minimum in the repulsive force occurring when the SiO_2 surface charge drops to zero at the iep. In this work, a silica probe is used to interrogate the surface of a TiO_2 electrode in aqueous solutions. Therefore, the pH-dependent surface charge of SiO_2 was checked to establish the probe surface potential. In a 10^{-3} M KCl aqueous solution at pH = 5.5, the SiO_2 surface potential was found to be −37 mV. This surface potential was determined by measuring the interaction force between the SiO_2 probe and a SiO_2 substrate and fitting this result to the electrostatic force model.[15]

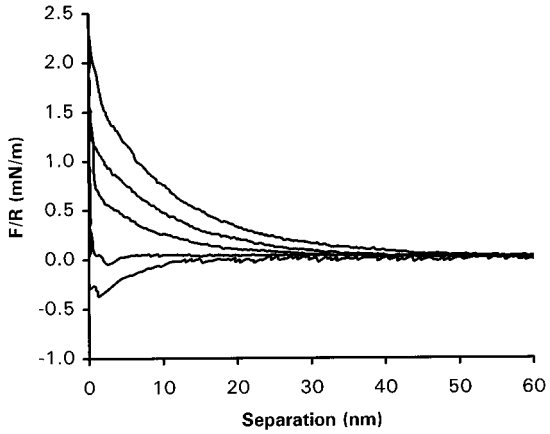

Figure 1. Forces between a silica probe and an n-type TiO_2 electrode in aqueous solution at 25 °C and open-circuit potential in 10^{-3} M KCl. The solution pH was adjusted by adding 0.01 M NaOH or 0.01 M HCl. Curves, from top to bottom, are for pH = 9.8, 8.5, 7.6, 5.7, and 3.4. The force is scaled to the probe radius of 10.5 μm.

The interaction between SiO_2 and undoped TiO_2 surfaces under open-circuit conditions has been examined previously.[6b,c] In the present work, an n-type TiO_2 electrode was examined. The interaction force between a SiO_2 probe tip and an n-TiO_2 electrode at open-circuit potentials is depicted in Figure 1. In a 10^{-3} M KCl solution, the force is repulsive at high pH (>5.7). This interaction becomes less repulsive with decreasing pH. Under these conditions, the Debye length was 10.2 nm and the interaction force decayed within the first 10−30 nm from the electrode surface.

As the solution pH is changed in these experiments, the charge on both the SiO_2 and TiO_2 surfaces is affected because of changes in the extent of protonation and deprotonation of surface groups. Under open-circuit conditions, the surface charge is determined solely by the coverage of OH^- and H^+ groups adsorbed to the metal (M) and metal oxide (MO) sites through the equilibrium relationships

$$M{-}OH + H^+ \rightleftarrows M{-}OH_2^+ \quad \text{and} \quad MO{-}H \rightleftarrows MO^- + H^+$$

At high pH values, the surface consists primarily of MO^- and M−OH sites, providing a negative surface charge. At low pH values, MO−H and $M{-}OH_2^+$ dominate to give a net positive surface charge. The pH at which the surface coverage of anionic and cationic groups is equal corresponds to the iep. For TiO_2 this occurs in the range of $5.2 < pH < 5.7$.[6b,c] In Figure 1, the iep for TiO_2 is observed at approximately pH 5.7. At this pH, the long-range electrostatic interaction is approximately zero, with a small attractive force appearing at small separations. This small attractive force is a combination of van der Waals attraction and a small electrostatic attraction due to the image charge on TiO_2 induced by the negatively charged SiO_2 probe.

In the absence of an external electric field, the diffuse double layer reflects the magnitude of adsorption-induced surface charges at the TiO_2 electrode. The application of an external electric field will produce additional charges at the electrode surface as the Fermi level of the TiO_2 shifts away from the flat-band potential. These charges are distributed throughout the space-charge layer of the semiconductor and result in conduction and valence band bending, upward for excess positive charge and downward for excess negative charge.[23]

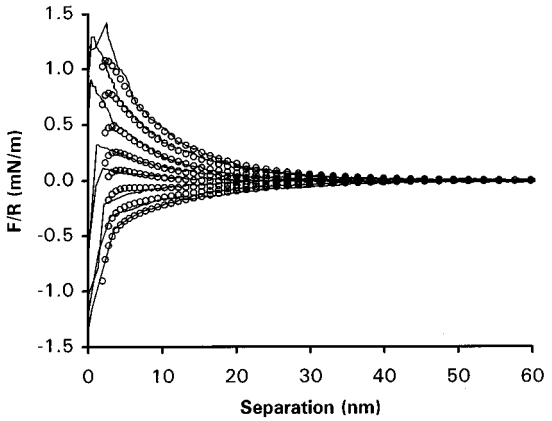

Figure 2. Measured (solid lines) force and theoretical fit (open circles) of interaction forces between SiO_2 probe and n-TiO_2 electrode as a function of the applied electrode potential at pH = 5.5 in a 10^{-3} M KCl aqueous solution. The electrode potentials are (from top to bottom) −0.90, −0.80, −0.70, −0.50, −0.43, −0.20, 0, and +0.50 V vs SCE. The theoretical fits correspond to a boundary condition of constant surface charge of −37 mV, $A_H = 1.4 \times 10^{-20}$ J, and a Debye length of $\kappa^{-1} = 10.2$ nm.

To illustrate this potential-dependent behavior, Figure 2 shows the interaction force between a SiO_2 probe and an n-TiO_2 electrode as a function of the potential applied to the TiO_2 when the solution (10^{-3} M KCl) is at pH 5.5, near the iep of TiO_2. The behavior of this substrate is similar to that observed for metals.[15] At negative electrode potentials, the n-TiO_2 possesses a negative surface charge. Unlike metals, however, where the charge is localized at the electrode surface, this charge is distributed over the space-charge layer and results in downward band bending near the semiconductor/electrolyte interface (Scheme 2A). The interaction force between the negatively charged SiO_2 probe and negatively charged TiO_2 electrode is purely repulsive under these conditions (Figure 2, upper curves). As the electrode potential is changed to more positive values, the electrode Fermi level moves downward and the extent of downward band bending decreases, resulting in a smaller repulsive force. At even larger positive potentials, an excess positive charge appears in the space-charge layer. This positive electrode charge results in upward band bending and a negatively charged ionic diffuse double layer in solution, producing an attractive electrostatic interaction with the positively charged ionic double layer of the SiO_2 probe. The measured interaction force saturates at sufficiently positive and negative electrode potentials, similar to previous results on metal electrodes.[14b,15]

The electrode potential at which the long-range electrostatic interaction between SiO_2 and n-type TiO_2 goes to zero (pzf) indicates the absence of surface charge on the electrode. Based upon visual inspection of the interaction curves in Figure 2, the pzf occurs at about −0.43 V vs SCE. Since these measurements were performed at the iep of TiO_2, the charge on the electrode is due solely to potential-induced electronic charges. Therefore, this potential can be identified as the V_{fb} at pH 5.5; at the iep, the pzf equals V_{fb}.

A more quantitative picture of the SiO_2−TiO_2 interaction can be obtained by fitting the experimental data to a theoretical description of the interaction force between two charged surfaces as above. In this analysis, the complete nonlinear Poisson−Boltzmann equation was solved to determine the potential distribution within the diffuse double layer while the SiO_2 and TiO_2 surfaces were held at constant surface charge. Generally, the boundary condition of assuming a constant surface charge provided a better fit than that assuming a constant surface potential, as in previous work with these systems.[6b,c] As stated earlier, this model ignores the potential drop through the space-charge layer. This is a reasonable assumption since the carrier density of this n-type TiO_2 was estimated to be 10^{19} cm^{-3}, as compared to that in a 10^{-3} M solution with a much smaller ion density of 12×10^{17} cm^{-3}. Therefore, most of the potential drop at the TiO_2/electrolyte interface occurs within the diffuse double layer and not in the space-charge layer. Moreover, near V_{fb} the potential drop within the space-charge layer disappears, and this simplified model converges to the complete solution. As the electrode potential is increased or decreased from this flat-band value, the specified surface potential of the semiconductor will deviate from the bulk potential.

SCHEME 2: Diagrams of Charge Distribution in Space-Charge Layer, Surface Adsorption Layer, and Diffuse Double Layer of a TiO_2 Electrode under Potential Control and the Corresponding Force Interactions with a Charged Silica Sphere in an Aqueous Solution

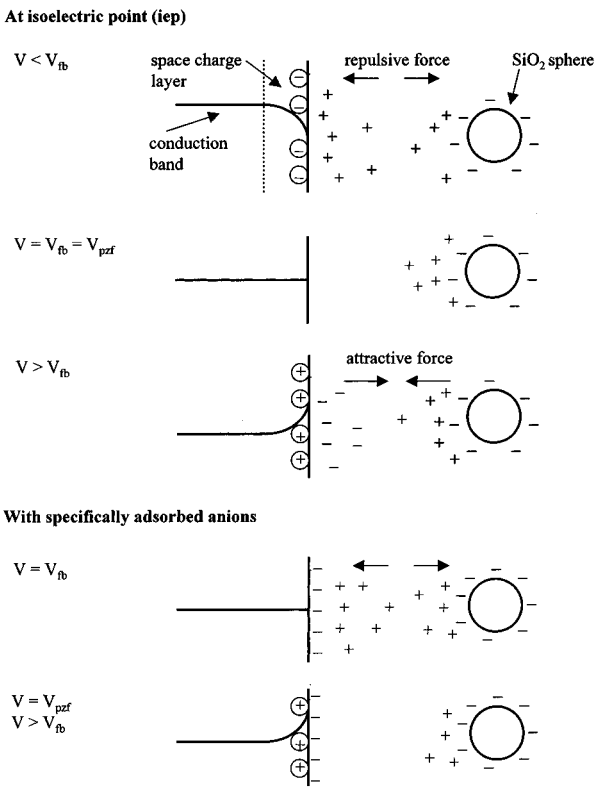

Fitting of the experimental force curves to this electrostatic model is illustrated in Figure 2 (open circles). These data were fit using a surface potential at infinite separation for the SiO_2 probe of −37 mV, as determined by force measurements between two SiO_2 surfaces, and a Debye length of 10.2 nm. As indicated in the figure, the theoretical curves fit the experimental force data quite well from large separation to a probe−substrate separation of 3−5 nm. Under repulsive conditions, which occur at negative electrode potentials, the predicted interaction force underestimates the measured repulsive interaction at small separations. This is attributed to an additional solvent force often observed in these measurements and also from the error associated with the true location of the surface charge on this electrode surface. The fit improves slightly under attractive conditions.

A summary of the surface potentials determined from these data by fitting the electrostatic force model is shown in Figure 3. The surface potential of TiO_2 varies from −47 mV at an electrode potential of −0.90 V vs SCE to +25 mV at an electrode potential of +0.50 V. The electrode potential at which the surface potential goes to zero occurs at about −0.45 V vs SCE. The surface potential increased from negative values at negative electrode potentials to positive values at positive

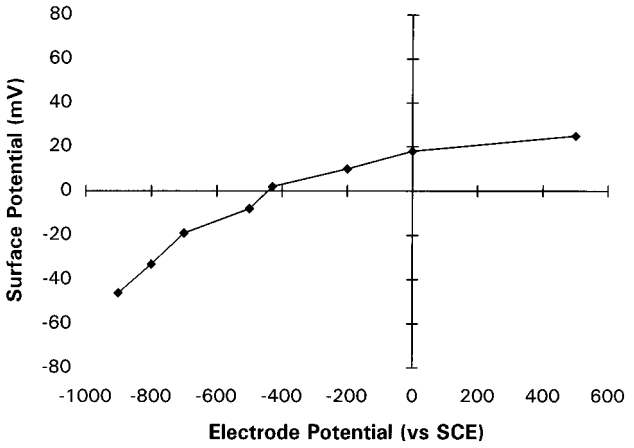

Figure 3. Surface potential of n-TiO_2 at infinite separation as a function of applied electrode potential vs SCE as determined by a best fit of the constant charge electrostatic model to experimental data in 10^{-3} M KCl. The electrode potential at zero surface charge is $\Psi_{pzc} = -0.45$ V in 10^{-3} M KCl.

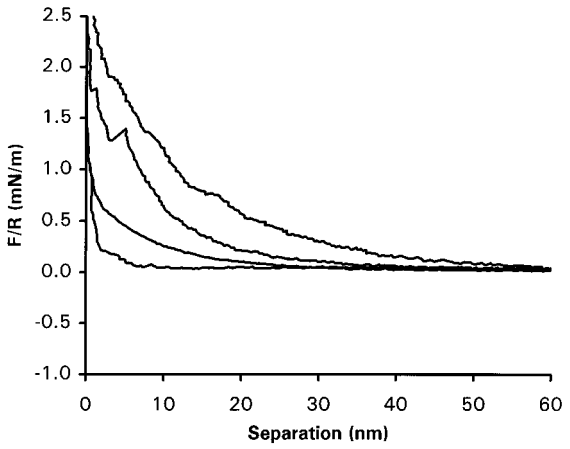

Figure 4. Forces between silica probe and n-TiO_2 electrode in aqueous solution at 25 °C and open-circuit potentials in a 10^{-3} M KCl aqueous solution containing 10^{-4} M HMP as a function of solution pH. From top to bottom, pH = 9.8, 7.6, 5.7, and 3.4. The force has been scaled to the probe radius of 10.5 μm.

electrode potentials. At positive surface potentials, corresponding to an attractive interaction between the SiO_2 probe and TiO_2 substrate, the accuracy of the surface potentials becomes questionable, because under attractive force conditions, the cantilever is unstable and exhibits a characteristic snap-in behavior.[2a] This limits the accuracy of force measurements in this regime.

At the iep, the surface charge on TiO_2 due to adsorbed species is zero, and the charge associated with the diffuse double layer is equal to the charge within the space-charge layer. Therefore, at the pzf both the charge in the diffuse double layer and the charge within the semiconductor are zero, so that this potential corresponds to V_{fb}. The V_{fb} in 10^{-3} M KCl, pH 5.5, at -0.45 V vs SCE is close to the V_{fb} determined using photocurrent onset methods, -0.40 V vs SCE.

Although TiO_2 is largely free from effects of specific adsorption of solution ions, changing the solution pH shifts V_{fb}, with an increase in pH shifting V_{fb} to more negative values, by 59 mV/pH unit.[23] The increased negative ionic charge on the semiconductor surface associated with an increase in the surface coverage of hydroxyl groups at higher pH tends to repel electrons from the surface region into the bulk. Thus, a more negative electrode potential is required to push these electrons back to the surface to achieve the flat-band condition. This increase in negative surface charge due to pH changes is shown in Figure 1 by an increase in the repulsive force at higher pH

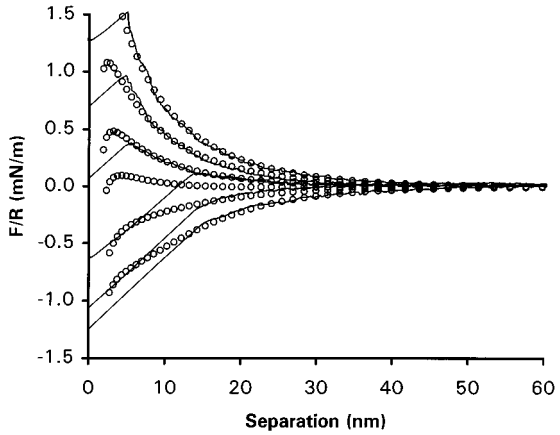

Figure 5. Measured (solid line) force and theoretical fit (open circles) of interaction between silica probe and n-TiO_2 electrode as a function of the electrode potential at pH = 5.5 in an aqueous solution of 10^{-3} M KCl containing 10^{-4} M HMP. The electrode potentials are (from top to bottom) -0.80, -0.60, -0.40, -0.21, 0, and $+0.50$ V vs SCE. The theoretical fits correspond to a boundary condition of constant surface charge and a Hamaker constant of 1.4×10^{-20} J.

values. Note that the observed effect also includes contributions from an increase in the surface charge of the SiO_2 probe. In addition to the hydroxyl anion, specific adsorption of Ti^{3+} occurs readily on TiO_2 and shifts V_{fb} toward more positive values.[24] The polymeric anion HMP strongly adsorbs on TiO_2 and should shift V_{fb} toward negative values. Indeed, the adsorption of HMP on TiO_2 influences the apparent surface charge. In Figure 4, a series of open-circuit force curves between SiO_2 and TiO_2 in a 10^{-3} M KCl aqueous solution in the presence of 10^{-4} M HMP indicates a greater repulsive force at a given pH value. For example, at pH 5.7 the SiO_2-TiO_2 interaction is noticeably more repulsive in the presence of HMP compared to a slightly attractive interaction at the same pH in the absence of HMP (see Figure 1). This indicates that the adsorption of HMP competes with the adsorption of OH^- to shift the iep of TiO_2 to lower pH values and increase the net negative surface charge. This increase in negative surface charge is consistent with the presumption that the flat-band potential also shifts toward more negative potentials.

To determine the location of the potential of zero force, a series of force curves were acquired on TiO_2 in the presence of HMP as a function of the applied electrode potential (Figure 5). These results indicate a trend in the interaction forces that is similar to the results observed in the absence of HMP. The TiO_2 surface is negatively charged at negative electrode potentials, and a repulsive force is observed. As the electrode potential is increased to more positive values, the interaction becomes attractive, indicating a change in sign of the charge associated with the diffuse double layer. A fit of the experimental data was again performed to determine the surface potential of the TiO_2 as a function of electrode potential. The theoretical curves in this case (Figure 5, open circles) fit the experimental data well in the repulsive regime, but the fit deteriorates as the attractive component in the interaction increases in magnitude. This lack of fit is partly due to the presence of an increasingly large snap-in component in the interaction forces. As was noted earlier, this snap-in occurs in the presence of attractive forces when the derivative of the interaction force exceeds the spring constant of the cantilever. Thus, the larger the attractive force, the earlier the snap-in condition occurs. The large snap-in distance observed for the $HMP-TiO_2$ surface suggests the presence of a longer range attractive force between tip and sample. This is likely a structural factor resulting from the polymeric nature of the HMP anion. If, rather than making a compact adsorbed layer on the

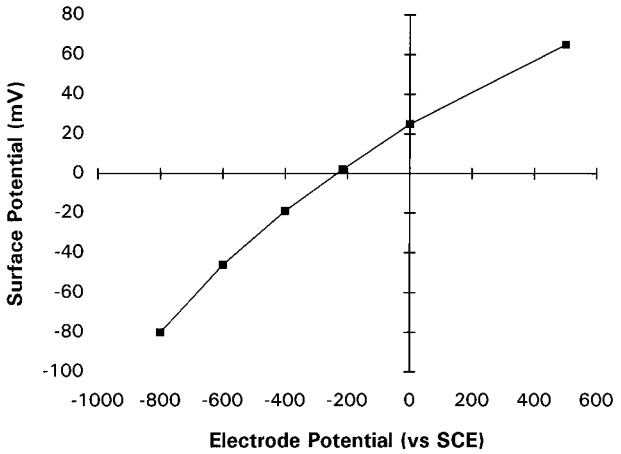

Figure 6. Surface potential of n-TiO_2 at infinite separation as a function of applied electrode potential vs SCE as determined by a best fit of the constant charge electrostatic model to experimental data in 10^{-3} M KCl with 10^{-4} M HMP (filled squares). The electrode potential at zero surface charge is $\Psi_{pzc} = -0.24$ V.

electrode, the HMP creates an extended layer with much of the charge residing directly at the surface but neutral long-chain species dangling into solution, electrostatic tip−substrate interactions would occur over their normal range, but attractive van der Waals interactions would appear at larger tip−sample separations and provide a stronger attractive force.

A compilation of the surface potentials for the TiO_2/HMP system indicates that the pzf shifts to more positive electrode potentials than was observed in the absence of HMP (Figure 6). These measurements show the pzf occurs at −0.24 V vs SCE, as compared to −0.45 V without HMP, in contrast to the shift in V_{fb}. The observed positive shift in the pzf is a consequence of the force measurements being governed by the charge of the diffuse double layer. In the absence of absorbed ions, the double-layer charge is a direct reflection of the potential-induced surface charges. However, when the TiO_2 surface deviates from the isoelectric point (Scheme 2B), either through changes in pH or due to adsorbed HMP, the charge of the double layer (σ_{dl}) reflects the sum of both potential-induced electronic (σ_p) and adsorption-induced ionic (σ_A) charges according to the relationship

$$\sigma_{dl} = \sigma_p + \sigma_A \qquad (5)$$

Thus, the presence of additional negative surface charge due to adsorbed species (σ_A) requires a more positive potential-induced charge (σ_p) to achieve a double-layer charge (σ_{dl}) of zero. By a similar argument, the flat-band potential under these conditions occurs when the potential-induced charge is zero and the double-layer charge equals the adsorption-induced ionic charge, which will be at more negative electrode potentials where the double-layer counterion charge is positive. Thus, at V_{fb} there will be a repulsive interaction with the SiO_2 probe.

Conclusions

The results presented here illustrate the influence of electrode potential and adsorbed species on diffuse double-layer formation at a semiconductor electrode. When TiO_2 is examined at its isoelectric point, the surface charge due to adsorbed species is zero, and the diffuse double layer is a direct reflection of the potential-induced charge in TiO_2. Therefore, the potential at which the diffuse double layer exhibits zero charge corresponds to the semiconductor flat-band potential. However, under conditions where TiO_2 is not at its isoelectric point, the diffuse double layer reflects a combination of potential-induced electronic surface charges and adsorption-induced ionic surface charges. Therefore, the condition of zero double-layer charge does not correspond to the flat-band potential. In fact, these two potentials shift in opposite directions. An increase in adsorbed negative charge shifts the flat-band potential to more negative electrode potentials while more positive electrode potentials are required to achieve pzf conditions. Therefore, force measurements cannot be used to directly determine the flat-band potential in the presence of charged adsorbates. However, with a sufficiently well-characterized probe, the surface charge due to adsorbed species can be measured at open circuit and subtracted from the potential-induced force curves to indirectly determine the flat-band condition.

Acknowledgment. Financial support from the Robert A. Welch Foundation and National Renewable Energy Laboratory is gratefully acknowledged.

References and Notes

(1) Israelachvili, J. N. *Intermolecular and Surface Forces*, 2nd ed.; Academic Press: New York, 1991.

(2) (a) Israelachvili, J. N.; Adams, G. E. *J. Chem. Soc., Faraday Trans. 1* **1978**, *74*, 975. (b) Parker, J. L.; Christenson, H. K.; Ninham, B. W. *Rev. Sci. Instrum.* **1989**, *60*, 3135.

(3) Claesson, P. M.; Ederth, T.; Bergeron, V.; Rutland, M. W. *Adv. Colloid Interface Sci.* **1996**, *67*, 119.

(4) For review see, for example: Butt, H.-J.; Jaschke, M.; Ducker, W. *Bioelectrochem. Bioenerg.* **1995**, *38*, 191.

(5) (a) Ducker, W. A.; Senden, T. J.; Pashley, R. M. *Nature* **1991**, *353*, 2239. (b) Ducker, W. A.; Senden, T. J.; Pashley, R. M. *Langmuir* **1992**, *8*, 1831.

(6) (a) Atkins, D. T.; Pashley, R. M. *Langmuir* **1993**, *9*, 2232. (b) Larson, I.; Drummond, C. J.; Chan, D. Y. C. *J. Am. Chem. Soc.* **1993**, *115*, 25. (c) Larson, I.; Drummond, C. J.; Chan, D. Y. C.; Grieser, F. *J. Phys. Chem.* **1995**, *99*, 2114.

(7) (a) Li, Y. Q.; Tao, N. J.; Pan, J.; Garcia, A. A.; Lindsay, S. M. *Langmuir* **1993**, *9*, 637. (b) Karaman, M. E.; Meagher, L.; Pashley, R. M. *Langmuir* **1993**, *9*, 1220. (d) Meagher, L.; Craig, V. S. J. *Langmuir* **1994**, *10*, 2736.

(8) (a) Biggs, S.; Chow, M. K.; Zukoski, C. F.; Grieser, F. *J. Colloid Interface Sci.* **1993**, *160*, 511. (b) Biggs, S.; Mulvaney, P. *J. Chem. Phys.* **1994**, *100*, 8501. (c) Biggs, S.; Mulvaney, P.; Zukoski, C. F.; Grieser, F. *J. Am. Chem. Soc.* **1994**, *116*, 9150.

(9) Rutland, M. W.; Senden, T. J. *Langmuir* **1993**, *9*, 412.

(10) (a) O'Shea, S. J.; Welland, M. E.; Rayment, T. *Langmuir* **1993**, *9*, 1826. (b) Rabinovich, Y. I.; Yoon, R.-H. *Langmuir* **1994**, *10*, 1903. (c) Biggs, S. *Langmuir* **1995**, *11*, 156.

(11) Derjaguin, B. V.; Voropayeva, T. N.; Kabanov, B. N.; Titiyevskaya, A. S. *J. Colloid Sci.* **1964**, *19*, 113.

(12) Fan, F.-R. F.; Bard, A. J. *J. Am. Chem. Soc.* **1987**, *109*, 6262.

(13) (a) Parker, J. L.; Christenson, H. K. *J. Chem. Phys.* **1988**, *88*, 8013. (b) Smith, C. P.; Maeda, M.; Atanososka, L.; White, H. S.; McClure, D. J. *J. Phys. Chem.* **1988**, *92*, 199.

(14) (a) Ishino, T.; Hieda, H.; Tanaka, K.; Gemma, N. *Jpn. J. Appl. Phys.* **1994**, *33*, L1552. (b) Raiteri, R.; Grattarola, M.; Butt, H.-J. *J. Phys. Chem.* **1996**, *100*, 16700.

(15) Hillier, A. C.; Kim, S.; Bard, A. J. *J. Phys. Chem.* **1996**, *100*, 18808.

(16) (a) Grahame, D. C. *Chem. Rev. (Washington, D.C.)* **1947**, *41*, 441. (b) Meites, L. *J. Am. Chem. Soc.* **1951**, *73*, 2035.

(17) (a) Clavilier, J.; Nguyen, V. H. *J. Electroanal. Chem.* **1973**, *41*, 193. (b) Tucceri, R. I.; Posadas, D. *J. Electroanal. Chem.* **1985**, *191*, 387. (c) Piela, B.; Wrona, P. K. *J. Electroanal. Chem.* **1995**, *388*, 69.

(18) (a) Cleveland, J. P.; Manne, S.; Bocek, D.; Hansma, P. K. *Rev. Sci. Instrum.* **1993**, *64*, 403. (b) Sader, J. E.; Larson, I.; Mulvaney, P.; White, L. R. *Rev. Sci. Instrum.* **1995**, *66*, 3789.

(19) (a) Derjaguin, B. *Trans. Faraday Soc.* **1940**, *36*, 203. (b) Derjaguin, B. V.; Landau, L. D. *Acta Phys. Chem.* **1941**, *14*, 633. (c) Derjaguin, B. V.; Landau, L. D. *J. Exp. Theor. Phys.* **1941**, *11*, 802. (d) Verway, E. J. W.; Overbeek, J. T. G. *Theory of the Stability of Lyophobic Colloids*; Elsevier: New York, 1948.

(20) Derjaguin, B. V. *Kolloid Z.* **1934**, *69*, 155.

(21) Parker, J. L. *Surf. Sci.* **1994**, *3*, 205.

(22) Grabbe, A.; Horn, R. G. *J. Colloid Interface Sci.* **1993**, *157*, 375.

(23) Finklea, H. O. In *Semiconductor Electrodes*; Finklea, H. O, Ed.; Elsevier: Amsterdam, 1988; pp 1−42.

(24) Ahmed, S. M.; Ahmed, A. In *Photoelectrochemistry: Fundamental Processes and Measurement Techniques*; Wallace, W. L., Nozik, A. J., Deb, S. K., Wilson, R. H., Eds.; The Electrochemical Society: Pennington, NJ, 1982; Proc. Vol. 82-3, pp 408−422.